Deflection Analysis of the Space Shuttle External Tank Door Drive Mechanism

Michael A. Tosto[*], Bo C. Trieu[**], Brent A. Evernden[+], Drew J. Hope,
Kenneth A. Wong and Robert E. Lindberg

Abstract

Upon observing an abnormal closure of the Space Shuttle's External Tank Doors (ETD), a dynamic model was created in MSC/ADAMS to conduct deflection analyses of the Door Drive Mechanism (DDM). For a similar analysis, the traditional approach would be to construct a full finite element model of the mechanism. The purpose of this paper is to describe an alternative approach that models the flexibility of the DDM using a lumped parameter approximation to capture the compliance of individual parts within the drive linkage. This approach allows for rapid construction of a dynamic model in a time-critical setting, while still retaining the appropriate equivalent stiffness of each linkage component. As a validation of these equivalent stiffnesses, finite element analysis (FEA) was used to iteratively update the model towards convergence. Following this analysis, deflections recovered from the dynamic model can be used to calculate stress and classify each component's deformation as either elastic or plastic. Based on the modeling assumptions used in this analysis and the maximum input forcing condition, two components in the DDM show a factor of safety less than or equal to 0.5. However, to accurately evaluate the induced stresses, additional mechanism rigging information would be necessary to characterize the input forcing conditions. This information would also allow for the classification of stresses as either elastic or plastic.

External Tank Door Background

The ETD cover openings in the Orbiter's underside, which are access regions for the umbilical and structural connections between the External Tank (ET) and Orbiter. The ETD sits at the aft underside of the Orbiter, and is prominently visible in its open configuration in Figure 1.

After jettisoning the ET during ascent, these doors are closed while on orbit and remain closed throughout the duration of flight and descent, until they are opened after landing for inspection. Proper door closure is critical to avoid excessive aero-heating during descent through the Earth's atmosphere. Thermal analysis has shown that if the doors are not fully closed and aligned with surrounding TPS tiles within 3.8 mm (0.15 in), a safe descent would be questionable [1].

The three main ETD subsystems are the Centerline Latches (CL), Door Drive Mechanism (DDM), and Uplatch Mechanism (UM). The CL locks the doors in their open configuration while the ET is connected to the Orbiter and throughout the ascent stage. With the ET jettisoned, and while in orbit, the DDM is commanded to move both doors from their open to closed configuration. Finally the UM, which has three hooks, is activated to latch the doors in their closed configuration and compresses the thermal and pressure seals for proper closure. Figure 2 shows a close-up of the starboard-side door with the DDM and the three hooks of the UM highlighted.

[*] National Institute of Aerospace/University of Virginia, Hampton, VA
[**] NASA Langley Research Center, Hampton, VA
[+] NASA Johnson Space Center, Houston, TX

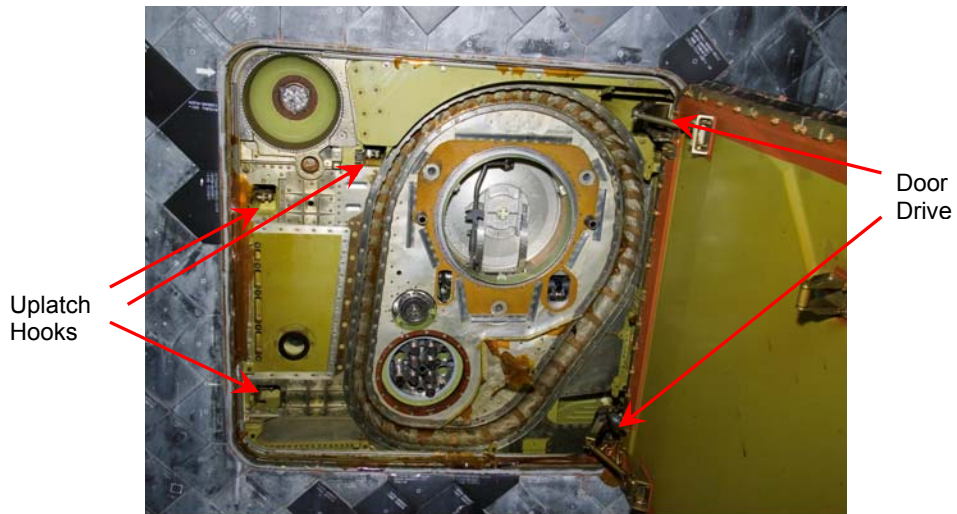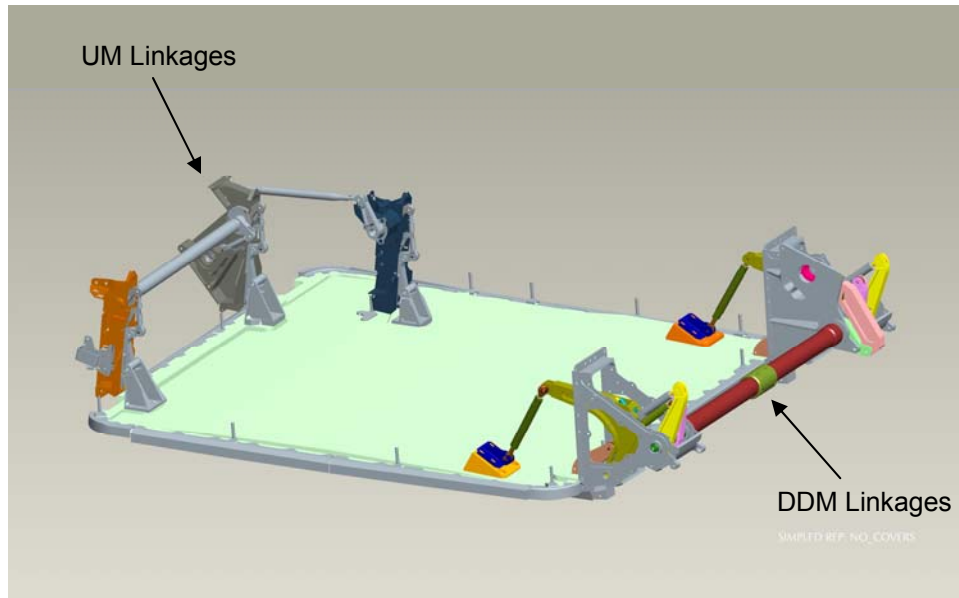**Figure 1. OV-103, *Discovery*, Before STS-114**

Figure 2. Close-Up of ETD Showing Uplatch Hooks and Door Drive

A Pro/E CAD model of the port-side ETD including the DDM and UM in its closed and latched configuration is shown in Figure 3. Actuators are not shown.

Figure 3. Port Side ET Door Configuration including DDM & UM

Analysis Approach

During the Space Shuttle mission STS-118 of August 2007, ground telemetry data indicated that the ETD did not fully complete their travel before the uplatches were commanded to engage. Because the DDM actuator has a fail-safe brake that engages when no power is applied, the mechanism is constrained at its input link as the door is forced to close. This constraint at the input link effectively creates deflection in the DDM linkages during uplatch operation and will therefore induce an associated stress.

FEA is frequently used to calculate stress for such loading conditions. Within this approach, a single analysis will describe the static loading of a given mechanism configuration. Additionally, the analyst must create a mesh of the entire mechanism, and then re-mesh for each configuration of interest. This process can be both labor intensive and time consuming, and most importantly, the mechanism dynamics are lost in such quasi-static analysis.

In this paper an alternative modeling approach is proposed for use in the multi-body dynamics software MSC/ADAMS. This approach utilizes lumped parameter approximations to model the compliance of individual parts within a mechanism. To represent each flexible part, single degree of freedom linear springs were introduced for links in tension and compression, while torsional springs at the base of rigid cranks were used for links in bending. With the door drive input crank fixed, the door was then forced to close, thereby simulating the conditions seen by the actual mechanism. To validate the representative equivalent stiffnesses, each was iteratively updated until convergence using the ratio of FEA stresses calculated based on spring deflection and spring force.

Modeling

Simulation to Obtain Deflections
Normal operation requires that two sets of indicators, at the uplatch hooks and in the door drive actuator, are both observed during door closure before running the uplatches. However, during the STS-118 mission only the first set of these indications was initially obtained. Therefore the door was within the

capture envelope of the UM (51 mm or 2 in from complete closure), but had not fully reached its intended latching location. Because the DDM's actuator brake is on during uplatch operation, the proposed analytical approach is used to find the induced deflections in the DDM linkages due to this unusually long uplatch stroke. Based on these deflections, or alternatively the associated spring forces, linkage stresses can be computed. For elastic deformations, cycling the ETD's DDM and UM mechanism will return the door to its final closed configuration with respect to the Shuttle as expected. If plastic deformations have occurred then the door may form gaps or a step with respect to the Shuttle.

The Pro/E model of the DDM shown in Figure 3 had been previously constructed at JSC and LaRC, and was used as a starting point for subsequent analysis. This model was imported into ADAMS, with the appropriate piece-parts merged into functional moving parts. As shown in Figure 4, the door rods within ADAMS are a simplified geometric representation of the actual linkage. For the purpose of the mechanism analyses, we chose to represent these links as rod elements with revolute joints at each end.
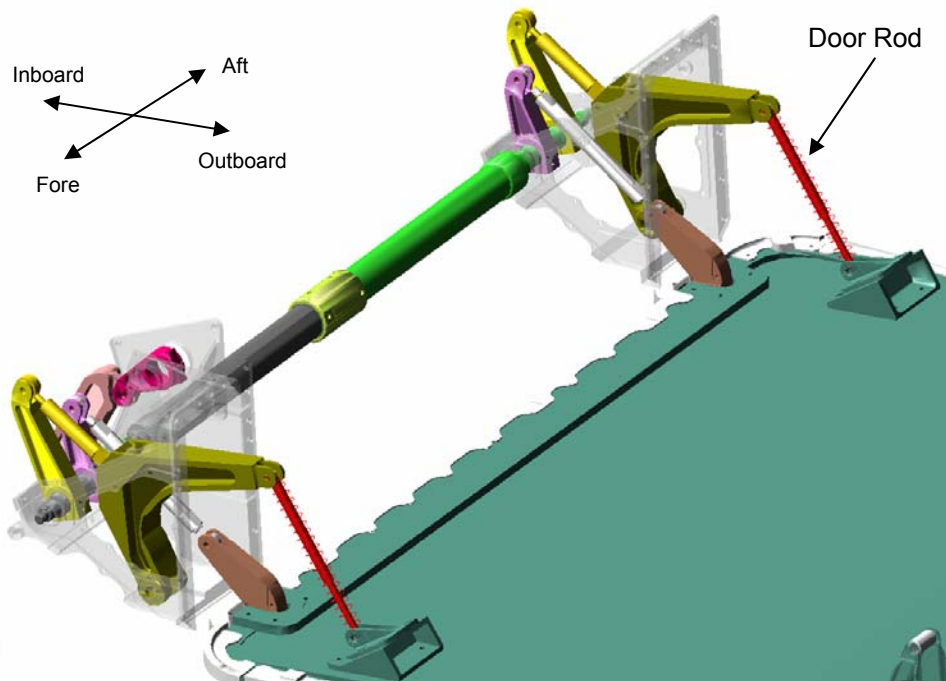
Figure 4. ETD Door Drive Mechanism

For deflection analyses, the linkages of the DDM are represented in ADAMS as spring or compliant members, while the door and shuttle frame are considered rigid. Figure 5 shows each part of the linkage and its spring equivalence depending on loading: linear springs are used for tension or compression and torsional springs (at the base of a rigid crank) for bending. For the "follower 1" part, both compression and bending loads exist, thus both linear and torsional springs are used respectively.
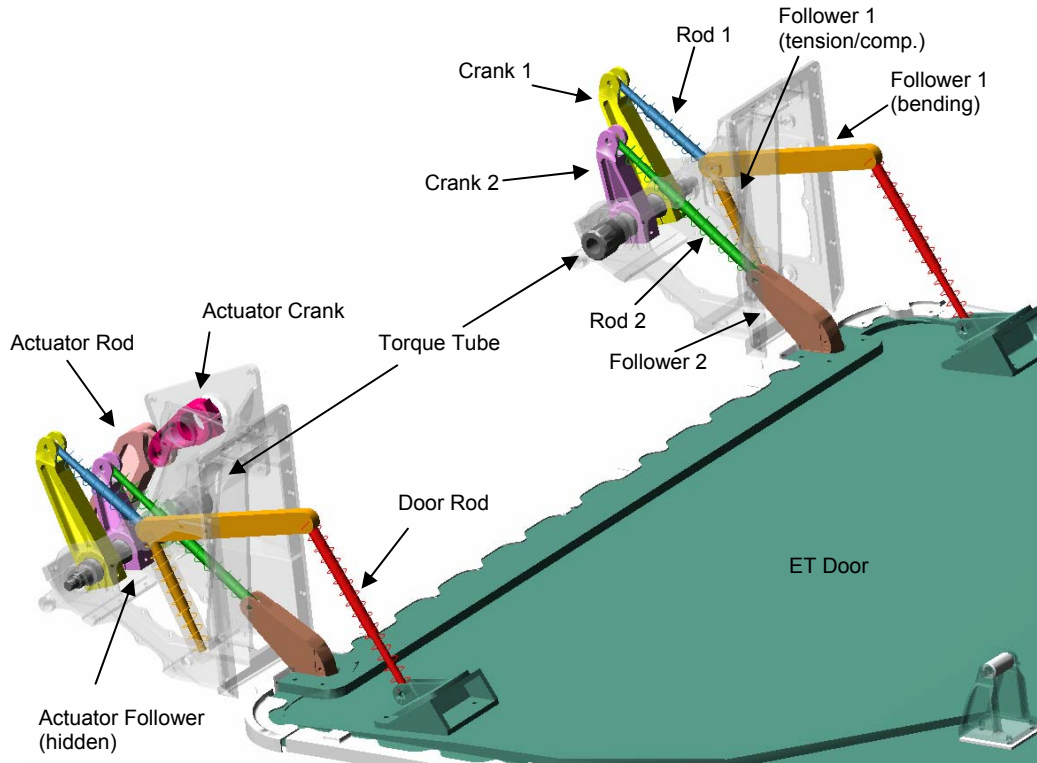
Figure 5. Spring/Compliant Representation of the DDM

To find initial equivalent stiffnesses for use in this lumped parameter model, a representative cross section of each part was taken near its midpoint and used to find values of cross sectional area (A) for linear springs and area moment of inertia (I) for torsional springs. Linear stiffness was found using equation (1) for a rod under axial load [2], and torsional stiffness was found using equation (2) for a cantilever beam with end load, assuming small deflections.

$$k_{eq} = \frac{EA}{l} \qquad \left[\frac{\text{N}}{\text{mm}} \right] \tag{1}$$

$$k_{eq} = l^2 \left(\frac{3EI}{l^3} \right) \left(\frac{\pi}{180} \right) \qquad \left[\frac{\text{N} \cdot \text{mm}}{\text{deg}} \right] \tag{2}$$

To run the dynamic simulation, the actuator crank is fixed (motor brake is on) while the opposing edge of the door is forced to move in the closing direction 25.4 mm (1 in). According to the door's rigging specifications, actuation of the DDM must leave the door between 25.4 mm (1 in) and 44.45 mm (1.75 in) of the fully closed and latched configuration under gravity [3]. Therefore, if the door were to stop short at 50.8 mm (2 in), then the maximum amount of additional displacement would be 25.4 mm, if the door were rigged to its minimum sag of 25.4 mm. Figure 6 shows this requirement, as presented in the ETD installation and rigging procedure [3].
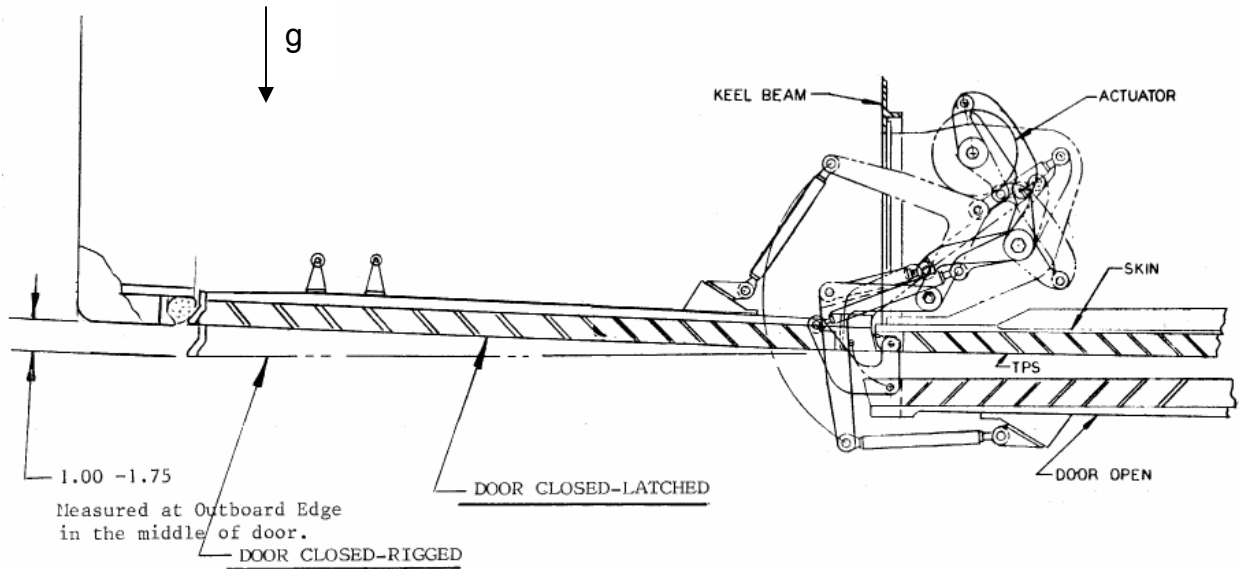
Figure 6. Port-side Door Looking FWD, Door Sag Specification

Iteration of Stiffness Approximations

If FEA is used to find stress in each component based on the results of dynamic simulation, this corresponds to a switch from a lumped parameter model in MSC/ADAMS to a distributed model in MSC/NASTRAN. While the resulting deflections and forces are analytic within ADAMS, where force and displacement for each link obey Hooke's law for a given equivalent stiffness, stresses computed in FEA using boundary conditions (BCs) based on these displacements and forces will be different unless the equivalent stiffness is the same in both models. In a linear static analysis, stress is proportional to force; therefore the ratio of stresses in these two load cases is equal to the ratio of applied force respectively. Equation (3) shows this relationship, where the subscript "disp" signifies an FEA model with displacement BCs, and "force" signifies an FEA model with force BCs. Similarly, subscripts "f" and "ds" indicate FEA and dynamic simulation respectively. After running an initial dynamic simulation and calculating the associated stresses, k_f is the only unknown in equation (3).

$$\frac{\sigma_{disp}}{\sigma_{force}} = \frac{F_{disp}}{F_{force}} = \frac{F_f}{F_{ds}} = \frac{k_f x_{ds}}{k_{ds} x_{ds}} \tag{3}$$

An iterative process is employed to ensure that the equivalent stiffnesses k_f and k_{ds} are in fact the same. By updating the value of k_{ds}, the stress ratio shown in equation (3) can be manipulated. When this ratio becomes equal to one, k_{ds} is therefore equal to the unchanged value of k_f. After an initial set of deflections and forces is obtained from the ADAMS model, these results are used as the input to a NASTRAN model of each flexible component. Using the stress ratio described above, a new equivalent stiffness for each link is computed according to equation (4). This result is then used to update the ADAMS model, thereby completing the loop of a process that can be repeated until convergence.

$$k_f = \left(\frac{\sigma_{disp}}{\sigma_{force}}\right) k_{ds} \quad \Rightarrow \quad k_{ds}[i+1] = \left(\frac{\sigma_{disp,i}}{\sigma_{force,i}}\right) k_i[i] \tag{4}$$

254

Results

Deflections

Table 1 shows the deflection of each part in the linkage from the initial iteration of ADAMS simulation. These deflections are used to compute the stress in each linkage member to classify it as either elastic or plastic deformation.

Table 1. Deflections in the DDM for 25.4 mm (1 in) at Door Edge

Linear Deflections				Angular Deflections		
Location	**Part**	**(mm)**		**Location**	**Part**	**(deg)**
Aft Hinge	Follower 1	5.67E-02		Aft Hinge	Follower 1	1.63E+00
	Rod 1	-3.05E-02			Crank 1	3.09E-01
	Rod 2	5.74E-02			Crank 2	-2.54E-01
	Door Rod	-1.74E-01		Fore Hinge	Follower 1	1.38E+00
Fore Hinge	Follower 1	4.80E-02			Crank 1	2.59E-01
	Rod 1	-2.57E-02			Crank 2	-4.76E-01
	Rod 2	1.08E-01		Actuator	Actuator Crank	-2.00E-01
	Door Rod	-1.48E-01			Actuator Follower	3.15E-01
Actuator	Actuator Rod	-2.23E-01		Torque Tube	Tube	-2.64E-01

(positive = tension, negative = compression)   (positive = fore [right hand rule])

Convergence of Equivalent Stiffness

Using the previously outlined process, stress ratios were calculated at iteration 0 and compared to the predicted stress ratio, calculated as a stiffness ratio. To find this stiffness ratio, the manually calculated approximate stiffness was used in place of k_{ds}, and a stiffness found directly from a finite element model (by applying a representative load of 4448 N (1000 lbf) and extracting the displacement) was used in place of k_f. These values are shown in the columns marked "K ratio [0]" in Table 2 and Table 3. Stress ratio values after one iteration, which should approach 1, are shown in the columns marked "σ ratio [1]".

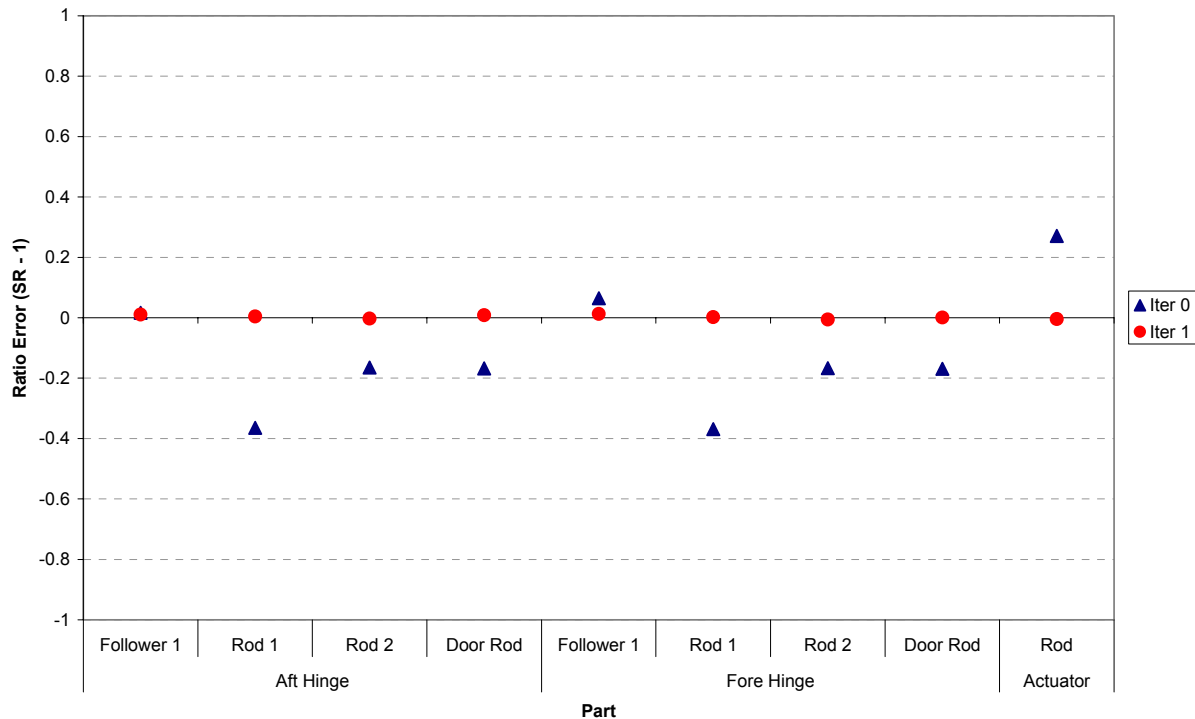**Table 2. Convergence of Stress Ratios, Links Axially Loaded**

Location	Part	K ratio[0]	σ ratio[0]	σ ratio[1]
Aft Hinge	Follower 1		1.016	1.011
	Rod 1	0.619	0.636	1.004
	Rod 2	0.829	0.835	0.997
	Door Rod	0.829	0.832	1.009
Fore Hinge	Follower 1		1.065	1.013
	Rod 1	0.619	0.632	1.002
	Rod 2	0.829	0.833	0.994
	Door Rod	0.829	0.831	1.001
Actuator	Rod		1.271	0.996

Table 3. Convergence of Stress Ratios, Links Loaded in Bending

Location	Part	K ratio[0]	σ ratio[0]	σ ratio[1]
Aft Hinge	Follower 1	1.701	1.806	1.061
	Crank 1	1.418	1.650	0.999
	Crank 2	1.491	1.624	1.005
Fore Hinge	Follower 1	1.701	1.793	1.062
	Crank 1	1.418	1.660	1.000
	Crank 2	1.491	1.630	1.007
Actuator	Crank	1.577	1.585	1.010
	Follower	1.549	1.415	1.062

Using these results, equivalent stiffnesses can be evaluated for convergence based on stress ratios. If the stress ratio is equal to 1 then the stiffness values used in ADAMS are equal to the equivalent stiffness of the part's finite element model. Therefore, a stress ratio error can be computed by subtracting 1 from all ratio values. As this stress ratio error approaches zero, the actual ratio will approach 1. Figure 7 and Figure 8 show the initial stress ratio error values at iteration 0, and the updated stress ratio error values after one iteration. Note that error values greater than 0 signify a part whose stiffness will be increased in the next iteration, while error values less than zero signify a part whose stiffness will be decreased in the next iteration.
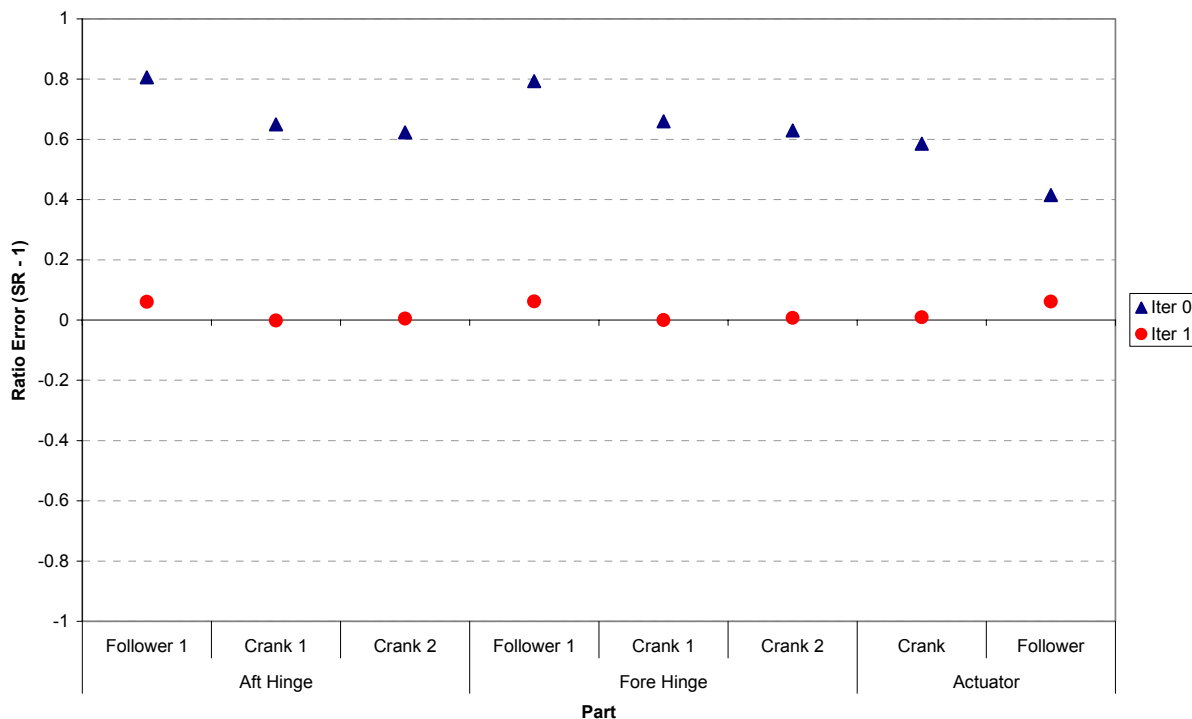

Figure 7. Stress Ratio in Parts Represented by Linear Springs

256

Torsional Springs, Stress Ratio Error

Figure 8. Stress Ratio in Parts Represented by Torsional Springs

Stress Analysis

The stress results for each component after one iteration (used to find the "σ ratio[1]" values in Table 2 and Table 3) are shown below in Table 4 and Table 5. These values represent the predicted stress induced by a 25.4 mm (1 in) forced movement of the door's outboard edge, with the DDM actuator crank fixed. To calculate factor of safety (FS) values, an allowable stress of 703 MPa (102 ksi) was used based on A286 stainless steel [4].

Table 4. Stress Results After 1 Iteration, Parts in Bending

Location	Part	Deflection (deg)	M (N·m)	F (N)	Displacement LBC FEA σ (MPa)	FS	Force LBC FEA σ (MPa)	FS	σ ratio[i]	σ ratio[i-1]
Aft Hinge	Follower 1	1.85E+00	2.34E+04	1.01E+05	1.44E+03	0.49	1.36E+03	0.52	1.061	1.806
	Crank 1	3.83E-01	2.27E+03	1.56E+04	5.12E+02	1.37	5.12E+02	1.37	0.999	1.650
	Crank 2	-3.15E-01	-2.38E+03	-2.45E+04	5.38E+02	1.31	5.36E+02	1.31	1.005	1.624
Fore Hinge	Follower 1	1.52E+00	1.92E+04	8.32E+04	1.19E+03	0.59	1.12E+03	0.63	1.062	1.793
	Crank 1	3.11E-01	1.84E+03	1.26E+04	4.16E+02	1.69	4.16E+02	1.69	1.000	1.660
	Crank 2	-5.87E-01	-4.43E+03	-4.56E+04	1.00E+03	0.70	9.93E+02	0.71	1.007	1.630
Actuator	Crank	-2.48E-01	-1.80E+03	-2.47E+04	6.52E+02	1.08	6.46E+02	1.09	1.010	1.585
	Follower	3.91E-01	2.71E+03	3.35E+04	9.51E+02	0.74	8.96E+02	0.78	1.062	1.415

Table 5. Stress Results After 1 Iteration, Parts in Tension/Compression

Location	Part	Deflection (mm)	F (N)	Displacement LBC FEA σ (psi)	FS	Force LBC FEA σ (psi)	FS	σ ratio[i]	σ ratio[i-1]
Aft Hinge	Follower 1	1.10E-01	8.42E+04	2.58E+02	2.73	2.55E+02	2.76	1.011	1.016
	Rod 1	-9.77E-02	-2.51E+04	3.48E+02	2.02	3.47E+02	2.03	1.004	0.636
	Rod 2	1.37E-01	3.41E+04	2.58E+02	2.73	2.59E+02	2.72	0.997	0.835
	Door Rod	-4.26E-01	-1.06E+05	8.07E+02	0.87	8.00E+02	0.88	1.009	0.832
Fore Hinge	Follower 1	9.00E-02	6.92E+04	2.12E+02	3.31	2.10E+02	3.36	1.013	1.065
	Rod 1	-7.99E-02	-2.06E+04	2.84E+02	2.48	2.83E+02	2.48	1.002	0.632
	Rod 2	2.55E-01	6.36E+04	4.78E+02	1.47	4.81E+02	1.46	0.994	0.833
	Door Rod	-3.50E-01	-8.72E+04	6.61E+02	1.06	6.60E+02	1.07	1.001	0.831
Actuator	Rod	-3.44E-01	-7.56E+04	1.73E+03	0.41	1.74E+03	0.40	0.996	1.271

Although these results do show some components with factors of safety less than one, this does not necessarily mean that closure of the ETD during STS-118 would have resulted in yield. Because the actual rigged door sag was not known at the time, this analysis did not produce a definitive prediction of additional stress induced in the door drive linkage. Because the minimum computed factor of safety for 25.4 mm (1 in) of door motion was 0.40, the door could be forced to move up to 10.16 mm (0.40 in) at its outboard edge before allowable stresses would be reached.

Conclusions

Through the use of MSC/ADAMS, a flexible multi-body dynamic simulation of the ETD DDM was quickly constructed and used to find linkage deflections. The advantage of this type of analysis is its relative simplicity compared to a full FEA model of the DDM, combined with preserved accuracy of mechanism kinematics. This simplicity allows for rapid construction of the model in addition to a reduction in computer computation time. Although complex geometry is reduced to lumped equivalent stiffnesses, the analyst has the ability to select each flexible degree of freedom that will be of primary interest and include it in the model. The stiffness used for each of these individual degrees of freedom may then be verified using FEA and iteratively updated as necessary.

The analysis shows that some components of the ETD have factors of safety less than one and may undergo plastic deformation. However, this is not conclusive because the forcing of the door is based on the worst case possible within rigging specifications. To complement the analyses described in this paper, actual rigging data from the Orbiter *Endeavour* taken before STS-118 could be used to reach a better estimate of stress in the DDM. Predicted stresses could then potentially be further confirmed through experimentation using a training mockup version of the DDM.

Acknowledgement

References

1. Don Picetti, Thermal Analysis and Test Results for ET Door Paint Striping, Boeing Orbiter Element, S063244, Daily PRCB Presentation
2. Rao, Singiresu S. Mechanical Vibrations, Fourth Edition, Pearson Prentice Hall, 2004
3. Brinkworth, D. "ET/Orbiter Umbilical Door Mechanism Installation and Rigging Procedure", Space Division Rockwell International, Doc. No. ML0308-0058 rev. C, 1982
4. MatWeb Material Property Data, http://www.matweb.com/search/DataSheet.aspx?MatID=13246&ckck=1